*Journal of Sound and Vibration* (2001) **248**(4), 621–634
doi:10.1006/jsvi.2001.3825, available online at http://www.idealibrary.com on IDEAL®

# ACOUSTIC TRANSMISSION ANALYSIS OF MULTI-LAYER ABSORBERS

F.-C. Lee and W.-H. Chen

*Department of Power Mechanical Engineering, National Tsing Hua University, Hsinchu, Taiwan* 30043, *Republic of China. E-mail: whchen@pme.nthu.edu.tw*

(*Received* 8 *November* 2000, *and in final form* 2 *April* 2001)

A simple but accurate analytical acoustic transmission analysis (ATA) is developed for evaluating the acoustic absorption of the multi-layer acoustic absorber. Unlike other analytical approaches available in literature, the present ATA can deal with the multi-layer acoustic absorber containing several compartments. Each compartment may include the layers of perforated plates, airspaces and porous materials together. The continuity of the particle velocity at the interfaces among perforated plates, airspaces and porous materials is assumed. The effects of the back surface acoustic impedance of both airspaces and porous materials are also taken into account. After combining those compartments, the resultant acoustic impedance and acoustic absorption coefficient of the multi-layer acoustic absorber can be obtained. For demonstration, four different types of multi-layer acoustic absorbers are analyzed. The results are also verified by relevant experiments or finite-element analysis. Finally, several important influence factors that affect the acoustic absorption of the multi-layer acoustic absorber are discussed.



## 1. INTRODUCTION

In recent years, noise control has received much attention for improving living environments. Multi-layer acoustic absorbers composed of perforated plates, airspaces or porous materials are commonly applied to absorb broadband noise. However, the acoustic absorption of these multi-layer acoustic absorbers is very dependent on their constructions. One of the objectives of this work is thus to develop an analytical method for the acoustic transmission analysis (ATA) of various multi-layer acoustic absorbers such that the factors that mainly influence the acoustic absorption can be verified distinctly.

Since the multi-layer acoustic absorber contains perforated plates, airspaces and porous materials, the acoustic properties of these materials need to be well simulated in the analysis. Beranek and Vér [1] presented a compact expression for the acoustic impedance of perforated plates. The expression indicated that the influence factors include the thickness, hole radius, hole pitch and porosity of the perforated plates and the air contained in the holes. As for porous materials, Delany and Bazley [2] stated that the complex wave propagation constant and characteristic impedance could be expressed in terms of the flow resistivity, wave number, air density and sound frequency. Qunli [3] provided an explicit proof to confirm the above empirical expression for the porous materials by a large amount of experimental data. Hence, based on those expressions [1, 2], one can clearly depict the acoustic properties of perforated plates and porous materials.

For the study of the multi-layer acoustic absorber in literature, Davern [4] presented an experimental study for a three-layer assembly which contains perforated plate, airspace and

0022-460X/01/490621 + 14 $35.00/0 

porous material respectively. The results indicated that the porosity of the perforated plate and the density of the porous material would considerably change the acoustic impedance and absorption coefficient of the acoustic absorber. In addition, only the frequency bands near the resonance frequency achieved high acoustic absorption. Dunn and Davern [5] provided an analytical analysis for the flat-walled anechoic lining composed of outer-, middle- and inner-layer porous materials. It was suggested that the outer-layer porous material with appropriate impedance should encourage the incident sound to enter the composite structure, but the inner-layer porous material was selected to attenuate the sound energy and prevent the incident sound from recombining. Jinkyo *et al.* [6] further studied the assembly with two layers of perforated plates backed with airspaces by an equivalent electrical circuit approach (EECA). The results showed that the assembly would have better acoustic absorption than that with single layer.

For practical multi-layer acoustic absorbers, a more complex assembly with more layers of perforated plates, airspaces and porous materials together is usually employed. However, by the analytical approaches [5, 6] mentioned above, the layers of perforated plates, airspaces and porous materials could not be tackled simultaneously. Thus, a new analytical acoustic transmission approach, which can be used to deal with practical multi-layer acoustic absorber containing several compartments, is developed in this work. In the present approach, each compartment may be composed of combinations of perforated plates, airspaces and porous materials together. The general versatility of the ATA is discussed. Relevant experiments or finite-element analysis are also performed to confirm the validity of the ATA. Some important acoustic features of the multi-layer acoustic absorber on the acoustic absorption are then presented in detail.

## 2. ACOUSTIC IMPEDANCE

Since the multi-layer acoustic absorber may consist of various combinations of perforated plates, airspaces or porous materials, the acoustic impedance of the $n$th layer of these components can be simulated and described as follows.

### 2.1. PERFORATED PLATES

The surface acoustic impedance of the $n$th layer of the perforated plates in low-sound pressure level without mean flow is given as [1]

$$\Gamma_{pn} = \frac{\rho_a}{\varepsilon_n}\sqrt{8\nu\omega}\left(1 + \frac{t_{pn}}{2a_n}\right) + \mathrm{i}\frac{\omega\rho_a}{\varepsilon_n}\left[\sqrt{\frac{8\nu}{\omega}}\left(1 + \frac{t_{pn}}{2a_n}\right) + t_{pn} + \delta_n\right], \tag{1}$$

where $\rho_a$ is the air density, $\nu$ is the kinematic viscosity of air ($\nu = 15 \times 10^{-6}$ m$^2$/s at room temperature), $\omega$ is the angular frequency and $\mathrm{i} = \sqrt{-1}$. $t_{pn}$, $a_n$, $\varepsilon_n$ ($= \pi a_n^2/b_n^2$) and $\delta_n$ ($= 0{\cdot}85(2a_n)\phi_n(\varepsilon_n)$) are the thickness, hole radius, porosity and viscous boundary layer thickness of the $n$th layer of the perforated plates respectively. $b_n$ is the hole pitch of the $n$th layer of the perforated plates and $\phi_n(\varepsilon_n) = 1 - 1{\cdot}47\sqrt{\varepsilon_n} + 0{\cdot}47\sqrt{\varepsilon_n^3}$.

### 2.2. POROUS MATERIALS

For homogeneous and isotropic porous materials, such as foams and fibrous materials, the acoustic impedance can be predicted by the useful empirical relations [2]. For the $n$th

layer of porous materials, the empirical relations for the complex wave propagation constant $\gamma_{mn}$ and characteristic impedance $Z_{mn}$ can be expressed by the flow resistivity $\sigma_n$ as

$$\gamma_{mn} = k_a \{c_{5n} (f\rho_a/\sigma_n)^{c_{6n}} + \mathrm{i}[1 + c_{7n} (f\rho_a/\sigma_n)^{c_{8n}}]\} \tag{2}$$

and

$$Z_{mn} = \rho_a c_a \{[1 + c_{1n} (f\rho_a/\sigma_n)^{c_{2n}}] - \mathrm{i}[c_{3n}(f\rho_a/\sigma_n)^{c_{4n}}]\}, \tag{3}$$

where $f$ is the sound frequency, $k_a = \omega/c_a$ is the wave number of air and $c_a$ is the sound speed of air. $c_{1n}, c_{2n}, \ldots, c_{8n}$ are the material constants for the $n$th layer of porous materials.

If the $n$th layer of porous materials is backed with a rigid wall, the surface acoustic impedance $\Gamma_{mn}$ of the $n$th layer of porous materials with the thickness $t_{mn}$ can be expressed as [5]

$$\Gamma_{mn} = Z_{mn} \coth(\gamma_{mn} t_{mn}). \tag{4}$$

### 2.3. AIRSPACES

Similar to porous materials, the complex wave propagation constant $\gamma_{an}$ and characteristic impedance $Z_{an}$ of airspaces can be found as

$$\gamma_{an} = \mathrm{i}k_a, \tag{5}$$

and

$$Z_{an} = \rho_a c_a. \tag{6}$$

If the $n$th layer of airspaces is backed with a rigid wall, the surface acoustic impedance $\Gamma_{an}$ of the $n$th layer of airspaces with the thickness $t_{an}$ can be expressed as [6]

$$\Gamma_{an} = -\mathrm{i}\rho_a c_a \cot(k_a t_{an}). \tag{7}$$

## 3. EQUIVALENT ELECTRICAL CIRCUIT APPROACH

In acoustic system analysis, the EECA [7] is one of the most popular approaches in literature. By using this approach, the sound pressure, particle velocity and acoustic impedance are respectively analogous to the voltage, electrical current and electrical impedance. Jinkyo *et al.* [6] applied this approach to calculate the resultant acoustic impedance $\Gamma_r$ of a multi-layer acoustic absorber composed of two layers of perforated plates backed with airspaces. In their procedure of calculating the resultant acoustic impedance $\Gamma_r$, the surface acoustic impedance of the inner perforated plate was first combined with the surface acoustic impedance of the back airspace in series connection and then recombined with the surface acoustic impedance of the front airspace in parallel connection. Finally, the above surface acoustic impedance was reconnected with the surface acoustic impedance of the outer perforated plate in series connection to obtain the resultant acoustic impedance $\Gamma_r$.

To evaluate the versatility of the concept of the equivalent electrical circuit approach in dealing with multi-layer acoustic absorbers, the approach is further generalized in this work. As shown in Figure 1, the second subscript number indicates the layer number and the innermost layers of the perforated plates and airspaces are defined as the first layers of

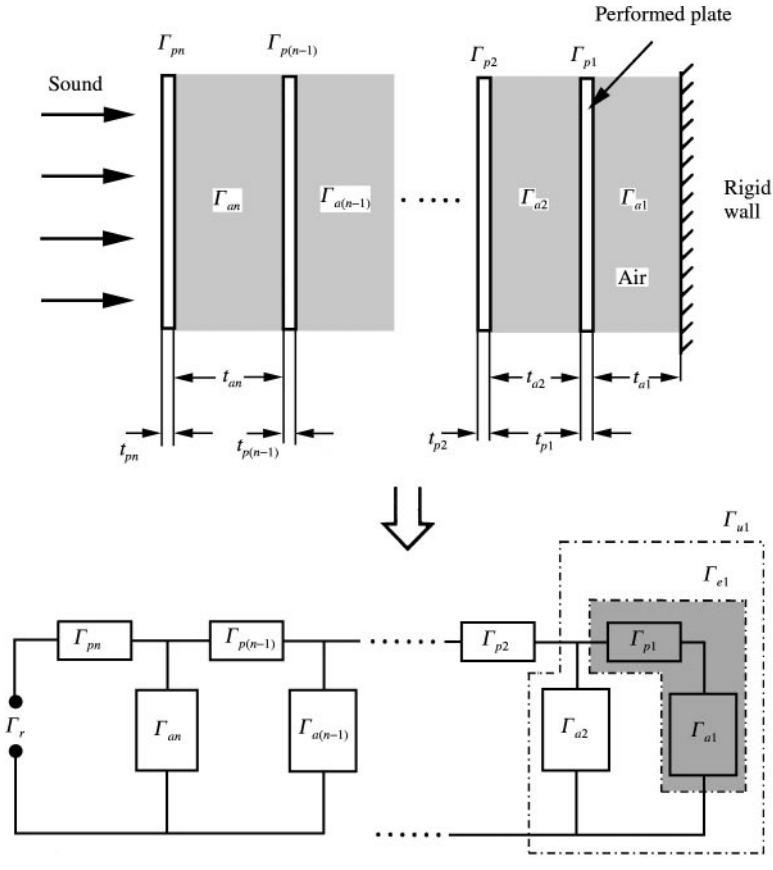


Figure 1. Generalization of the equivalent electrical circuit approach.

the perforated plates and airspaces respectively. Owing to the continuity of the particle velocity, the equivalent acoustic impedance $\Gamma_{e1}$ of the first layers of the perforated plates and airspaces (backed with rigid wall) can thus be regarded as the surface acoustic impedance of the perforated plate and back airspace in series connection [6], say,

$$\Gamma_{e1} = \Gamma_{p1} + \Gamma_{a1}, \tag{8}$$

where $\Gamma_{p1}$ and $\Gamma_{a1}$ are the surface acoustic impedance of the first layers of the perforated plates and airspaces (backed with a rigid wall), which can be obtained from equations (1) and (7) respectively. Next, due to the continuity of sound pressure, the equivalent acoustic impedance $\Gamma_{e1}$ can be considered to be in parallel connection with the surface acoustic impedance $\Gamma_{a2}$ of the second layer of the airspaces, which can also be obtained from equation (7). Therefore, the equivalent acoustic impedance $\Gamma_{u1}$ induced by the first layers of perforated plates and airspaces and the second layer of the airspaces can be expressed as

$$\Gamma_{u1} = \frac{\Gamma_{a2}\,\Gamma_{e1}}{\Gamma_{a2} + \Gamma_{e1}}. \tag{9}$$

Continuing the same procedures successively, the resultant acoustic impedance $\Gamma_r$ of the multi-layer acoustic absorber can be evaluated. In addition, the acoustic absorption

coefficient $\alpha$ of the multi-layer acoustic absorber can be obtained from the resultant acoustic impedance $\Gamma_r$ as [6]

$$\alpha = \frac{4R_r/\rho_a c_a}{(R_r/\rho_a c_a + 1)^2 + (X_r/\rho_a c_a)^2}, \tag{10}$$

where $R_r$ and $X_r$ denote the real and imaginary parts of the resultant acoustic impedance $\Gamma_r$ respectively.

By the EECA, it is noted that the surface acoustic impedance of back airspaces is assumed as the acoustic impedance of rigid wall even when the airspace is actually backed with perforated plates. Besides, the analysis is limited to the case with only one airspace existing in the space between adjacent perforated plates. Hence, for a more practical assembly of multi-layer acoustic absorbers, a versatile acoustic transmission analysis is necessary and will be presented in the following section.

## 4. ACOUSTIC TRANSMISSION ANALYSIS

For practical multi-layer acoustic absorbers, various combinations of perforated plates, airspaces and porous materials are involved. The effects of the back surface acoustic impedance of both airspaces and porous materials should be considered. The scheme of the ATA is displayed in Figure 2, where $\Gamma_{jn}$ ($j = a$ or $m$) represents the surface acoustic impedance of the $n$th layer of airspaces or porous materials. The multi-layer acoustic absorber discussed can be divided into several compartments by perforated plates. Without loss of generality, each compartment is composed of one layer of perforated plate and several layers of airspaces and porous materials. The innermost layers of the perforated plates, airspaces and porous materials are defined as the first layers of the perforated plates, airspaces and porous materials respectively.

For the first compartment, the surface acoustic impedance $\Gamma_{j1}$ ($j = a$ or $m$) of the first layer of airspaces or porous materials can be represented by [5]

$$\Gamma_{j1} = Z_{j1} \frac{Z_r \cosh(\gamma_{j1} t_{j1}) + Z_{j1} \sinh(\gamma_{j1} t_{j1})}{Z_r \sinh(\gamma_{j1} t_{j1}) + Z_{j1} \cosh(\gamma_{j1} t_{j1})} \quad (j = a \text{ or } m), \tag{11}$$

where $Z_r$ is the back surface acoustic impedance of the first layer of airspaces or porous materials backed with a rigid wall, and is taken as $\infty$. Similarly, the surface acoustic impedance of the next layer of airspaces or porous materials can also be evaluated by equation (11) except that the back surface acoustic impedance $Z_r$ is substituted by the surface acoustic impedance $\Gamma_{j1}$ ($j = a$ or $m$). Thus, the effects of various combinations of airspaces and porous materials between adjacent perforated plates can be accurately described in the same way.

Since the complex wave propagation constant and characteristic impedance are only employed for homogeneous and isotropic materials in sound propagation, the acoustic properties of perforated plates are not described by these two parameters [3]. Therefore, the combination of the surface acoustic impedance of the perforated plates and airspaces or porous materials cannot be tackled by the above procedure. It is assumed that as the incident sound passes through the holes of the perforated plate and is immediately transmitted to the airspace or porous material behind the perforated plate, the particle velocity is almost not abated [7]. The continuity of the particle velocity is thus adopted in this work to combine the surface acoustic impedance of the perforated plates and airspaces

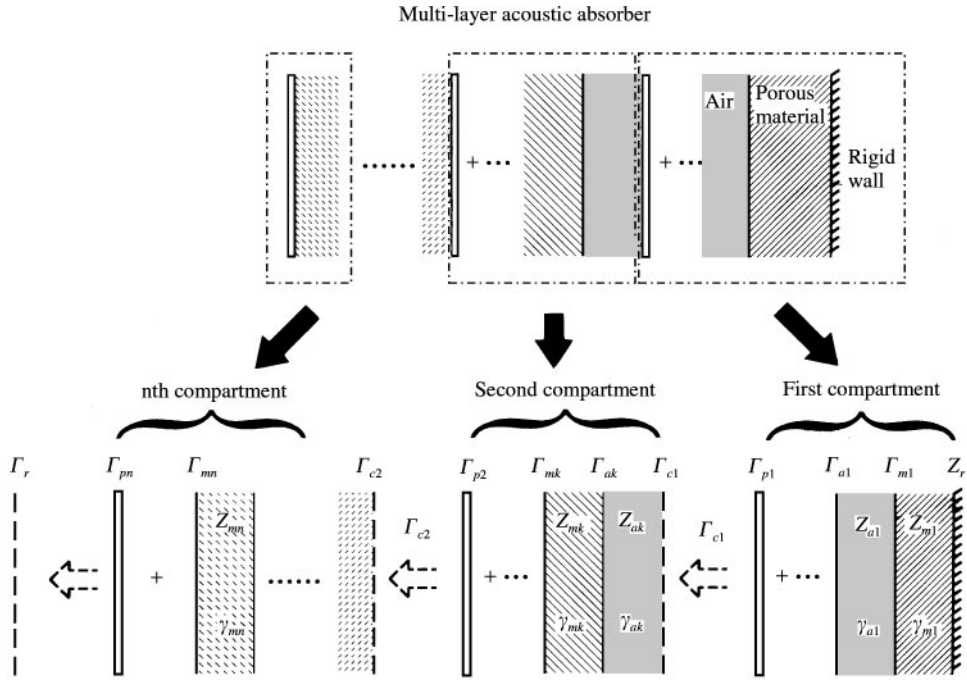


Figure 2. The acoustic transmission analysis.

or porous materials. The surface acoustic impedance $\Gamma_{c1}$ of the first compartment can be evaluated by the surface acoustic impedance of the first layer of the perforated plates $\Gamma_{p1}$ and the $(k-1)$th layer of the airspaces or porous materials $\Gamma_{j(k-1)}$ ($j = a$ or $m$) as

$$\Gamma_{c1} = \Gamma_{p1} + \Gamma_{j(k-1)} \quad (j = a \text{ or } m). \tag{12}$$

Now, for the next calculation, the surface acoustic impedance $\Gamma_{c1}$ of the first compartment can be treated as the back surface acoustic impedance of the first layer or airspaces or porous materials of the second compartment. This compensates the drawback of the equivalent electrical circuit approach, which always assumes the back surface acoustic impedance of airspaces or porous materials as that of the rigid wall even when the airspaces or porous materials are actually backed with the perforated plate. Consequently, the resultant acoustic impedance $\Gamma_r$ of the practical multi-layer acoustic absorber can be evaluated by the present ATA and then the acoustic absorption coefficient $\alpha$ can also be computed by equation (10).

## 5. EXPERIMENTS

The two-microphone impedance tube system [8] is used to measure the acoustic absorption coefficient $\alpha$ of the multi-layer acoustic absorbers studied. The configuration of the two-microphone impedance tube system is shown in Figure 3. The components of the system mainly include the following. [9]

(1) The impedance tube, which contains two pieces of 1/2″ microphones (B&k 4133 type) and a speaker. The acoustic absorber sample is set up inside the impedance tube.

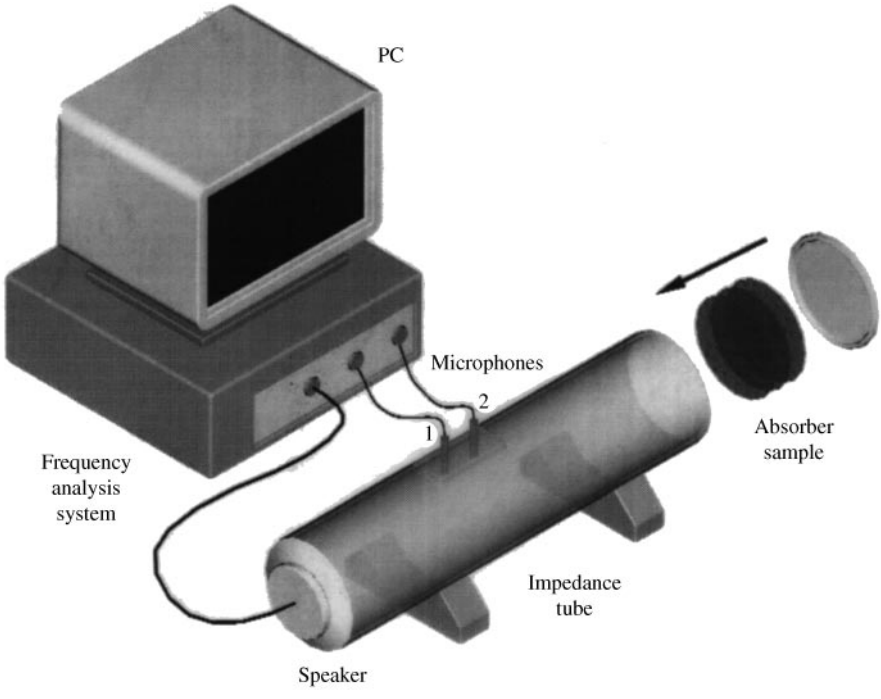


Figure 3. Configuration of the two-microphone impedance tube system.

(2) The personal computer system, which includes the frequency analysis system (Norwegian 830 type) and acoustic signal driver. A random noise is driven by the acoustic signal driver and transmitted into the impedance tube. By the two microphones in the impedance tube and the frequency analysis system, the transfer function $H_{21}$ ( $= p_2/p_1$) can be obtained. $p_1$ and $p_2$ are, respectively, the sound pressures measured by the first and second microphones. The experimental acoustic absorption coefficient $\alpha$ of the acoustic absorber sample can then be calculated by [9]

$$\alpha = 1 - \left| \frac{H_{21} - e^{-ik_a(z_1 - z_2)}}{e^{ik_a(z_1 - z_2)} - H_{21}} e^{i2k_a z_1} \right|^2, \tag{13}$$

where $z_1$ ($z_2$) denotes the distance between the first (second) microphone and the acoustic absorber sample.

During the measurement of the acoustic absorption coefficient $\alpha$ of the acoustic absorber samples, the upper-limited frequency $f_m$, which is the cut-off frequency of a non-planar mode of propagation, is of critical concern. $f_m$ should be $< 0{\cdot}586c_a/d$ to insure that the plane wave is transmitted in the impedance tube, $d$ denoting the diameter of the impedance tube. In addition, the distance between the first and second microphones must be less than $c_a/2f_m$ [8], which is taken as 5 cm in our system. The range of measured frequency is 100–2000 Hz and the acoustic absorption coefficient $\alpha$ is calculated with an interval of 5 Hz. Since the transfer function estimates are based on sample records of finite duration (about 15 s in our measurement) and finite frequency resolution (5 Hz), they are sensitive to random and bias errors [8]. To reduce the random errors, ensemble averaging (measuring five individual estimates and evaluating the average) or frequency smoothing (averaging the

results for five frequency bands) is adopted. Bias errors will be reduced when the time length of each sample record (about 40 ms) is much larger than the acoustic propagation time $2d_s/c_a$ (about 1·75 ms) within the impedance tube; $d_s$ ( = 0·3 m) is the distance from the first microphone to the end of the tube where the absorber sample is located.

## 6. RESULTS AND DISCUSSIONS

To validate the accuracy of the ATA developed, four cases are considered. The assembly with two layers of perforated plates backed with airspaces, which has also been solved by Jinkyo *et al.* [6] using the EECA, is first tackled. The porosity of the perforated plates $\varepsilon_1 = 2\%$ and $\varepsilon_2 = 1\%$, thickness $t_{p1} = t_{p2} = 20$ mm, hole radius $a_1 = a_2 = 2$ mm, and thickness of airspaces $t_{a1} = 600$ mm and $t_{a2} = 300$ mm are taken the same as those by Jinkyo *et al.* [6]. Figure 4 shows that the computed acoustic absorption coefficients of the present ATA agree well with those of Jinkyo *et al.* [6] by both the experiment and EECA. The second case studied is the assembly with three layers of perforated plates backed with airspaces. The thickness of perforated plates $t_{p1} = t_{p2} = t_{p3} = 1$ mm, thickness of airspaces $t_{a1} = t_{a2} = t_{a3} = 39$ mm, hole pitch $b_1 = b_2 = b_3 = 6$ mm, and hole radius $a_1 = 0{\cdot}5$ mm, $a_2 = 0{\cdot}75$ mm and $a_3 = 1$ mm. Thus, the porosity of the perforated plates is found to be $\varepsilon_1 = 2{\cdot}2\%$, $\varepsilon_2 = 4{\cdot}9\%$ and $\varepsilon_3 = 8{\cdot}7\%$ respectively. Figure 5 reveals that the results of the present ATA also agree reasonably well with the experimental data by the two-microphone impedance tube system. However, the results by the EECA are completely different. As mentioned earlier, this may be attributed to the assumption that the back surface acoustic impedance of the airspace in the EECA is considered as the acoustic impedance of the rigid wall when the airspace is backed with the perforated plate as seen in Figure 5. From Figures 4 and 5, unlike the EECA, the present ATA also achieves good results for the analysis of the assembly with three layers of perforated plates backed with airspaces.

To estimate the versatility of the present ATA for the multi-layer acoustic absorbers involving the perforated plates, porous materials and airspaces together, the third case which has been experimentally studied by Davern [4] is demonstrated in Figure 6. As seen

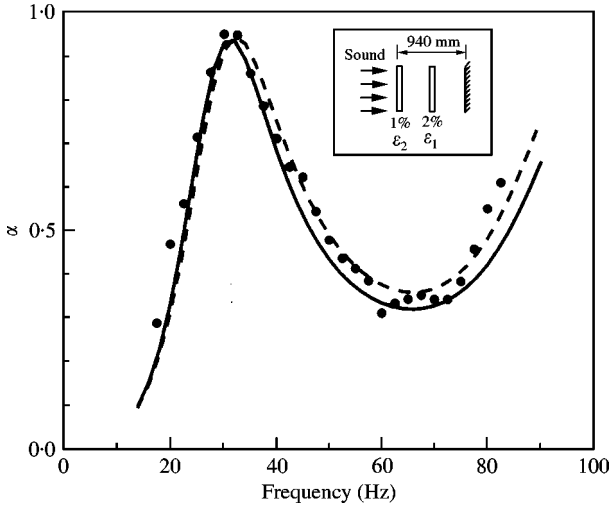


Figure 4. Comparison of the acoustic absorption coefficients for the assembly with two layers of perforated plates backed with airspaces. Present: ——, ATA, Jinkyo *et al.* [6]: – – –, EECA; ●, experiment.

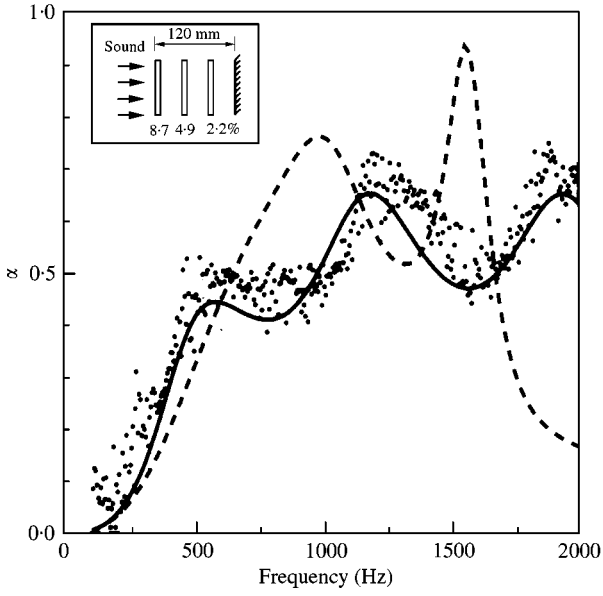


Figure 5. Comparison of the acoustic absorption coefficients for the assembly with three layers of perforated plates backed with airspaces. Present: ——, ATA; ····, experiment; – –, EECA.

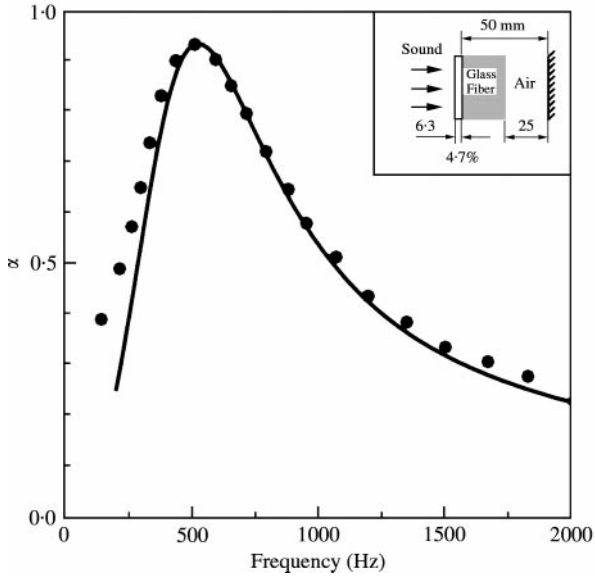


Figure 6. Comparison of the acoustic absorption coefficients for the assembly with perforated plate, glass fiber material and airspace. Present: ——, ATA. Davern [4]: ●, experiment.

from Figure 6, the results of the present ATA agree well with the experimental data provided by Davern [4]. From Figures 5 and 6, when the layers of perforated plates increase, the difference between the experimental data and calculated results also rises. This may be induced from the inevitable disagreement between the calculated surface acoustic

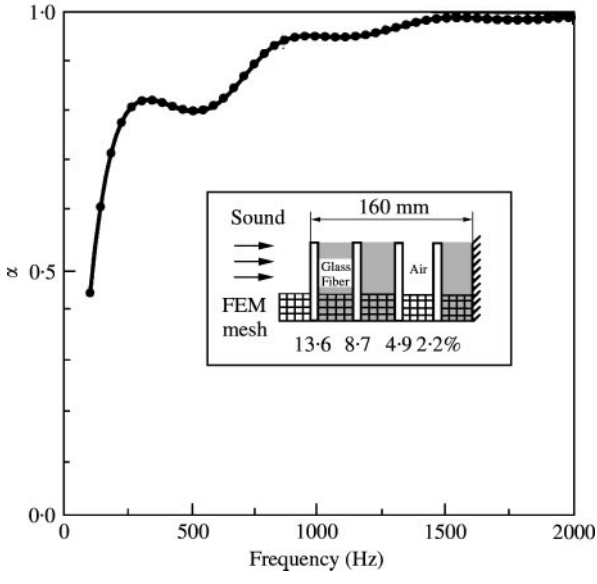


Figure 7. Comparison of the acoustic absorption coefficients for the random assembly with perforated plates, glass fiber materials and airspace. Present: ——, ATA; ····, FEM.

impedance of the perforated plates and the acoustic characteristics of practical perforated plates.

To further validate the flexibility of the ATA, the random assembly with perforated plates, airspaces and porous materials, as presented in Figure 7, is discussed. In this case, except for $t_{p4} = 1$ mm, $t_{a4} = 39$ mm, $b_4 = 6$ mm, $a_4 = 1{\cdot}25$ mm, $\varepsilon_4 = 13{\cdot}6\%$ and flow resistivity of glass fiber materials $\sigma = 16\,000$ Ns/m$^4$, all the parameters are the same as in the second case. Figure 7 depicts that the results obtained by the ATA are well consistent with those of finite-element solutions [10, 11]. That is, the ATA is also applicable even for the analysis of the random assembly with over three layers of perforated plates backed with porous materials and airspace.

To study the acoustic characteristics of multi-layer acoustic absorbers, the assemblies with three layers of perforated plates backed with airspaces or porous materials are also analyzed by the present ATA in the following sections.

### 6.1. VARIATION OF THE ACOUSTIC RESONANCE FREQUENCY

Herein, the acoustic resonance frequencies of the multi-layer acoustic absorber and its compartments are discussed. The multi-layer acoustic absorber solved here contains three compartments, where each compartment is composed of one layer of perforated plate and airspace. The geometric parameters are that the thickness of perforated plates $t_{p1} = t_{p2} = t_{p3} = 1$ mm, thickness of airspaces $t_{a1} = t_{a2} = t_{a3} = 19$ mm, hole pitch $b_1 = b_2 = b_3 = 6$ mm, hole radius $a_1 = 0{\cdot}5$ mm, $a_2 = 0{\cdot}75$ mm and $a_3 = 1$ mm, and the porosity of perforated plates $\varepsilon_1 = 2{\cdot}2\%$, $\varepsilon_2 = 4{\cdot}9\%$ and $\varepsilon_3 = 8{\cdot}7\%$. Figure 8 reveals that the acoustic resonance frequencies of this multi-layer acoustic absorber are more broadband than those of their individual compartments. The lowest and highest acoustic resonance frequencies of this multi-layer acoustic absorber are respectively lower and higher than

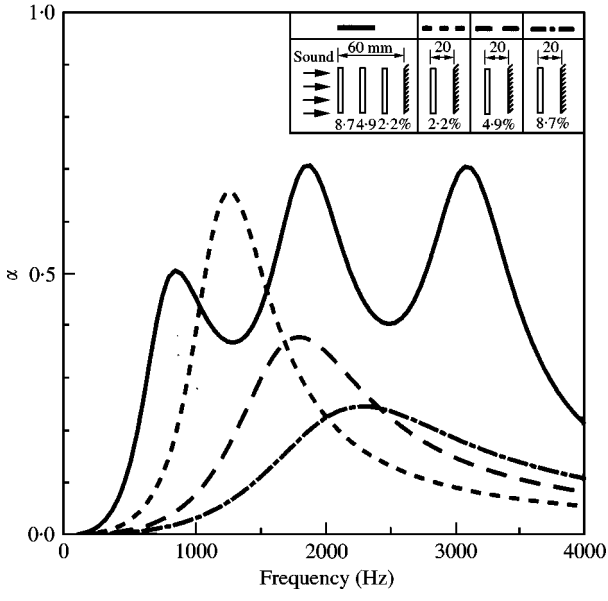


Figure 8. Variation of the acoustic resonance frequencies of the multi-layer acoustic absorber and its compartments.

those of their individual compartments. It is noted that the lower porosity of the perforated plate has a lower acoustic resonance frequency and higher acoustic absorption effect. In addition, when the incident frequency is equal to the acoustic resonance frequency of the multi-layer acoustic absorber, the medium existing in the acoustic absorber will vibrate with the incident sound and the incident sound energy will be largely absorbed. Hence, as seen in Figure 8, the acoustic absorber shows better acoustic absorption at the acoustic resonance frequency.

### 6.2. EFFECT OF MULTI-LAYER PERFORATED PLATES

For studying the effect of multi-layer perforated plates, the acoustic absorbers with three- or single-layer perforated plates backed with airspaces are solved. The geometric parameters shown in Figure 9 are the same as the multi-layer acoustic absorber discussed in the last section except for the thickness of airspaces for the cases with single layer of perforated plate backed with airspace. Apparently, for the present cases with single layer of perforated plate backed with airspace, there are two acoustic resonance frequencies are observed instead of one. Besides, the lower porosity of the perforated plate has better acoustic absorption at lower frequency bands. However, the higher porosity of the perforated plate demonstrates more broadband absorption ranges at higher frequency bands. For the assembly with three layers of perforated plates backed with airspaces, the acoustic absorption is generally more broadband and better than that with single layer of perforated plate backed with airspace.

### 6.3. EFFECT OF ARRANGEMENT OF PERFORATED PLATES

The effect of different arrangements of perforated plates in the multi-layer acoustic absorber on the absorption coefficient is then discussed. As shown in Figure 10, both the

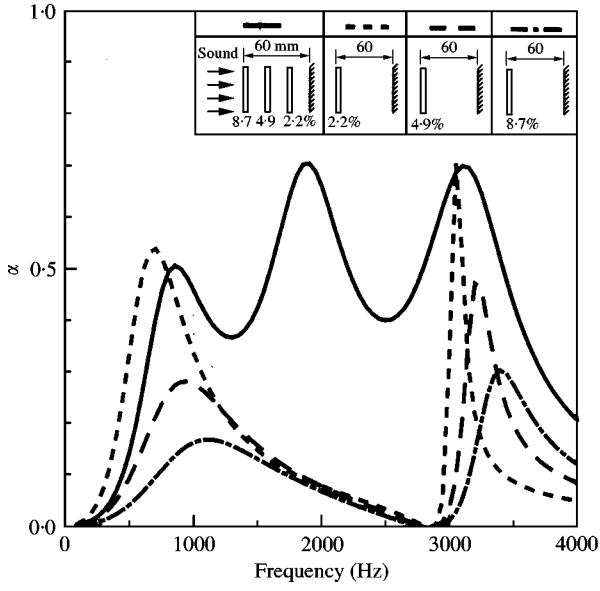


Figure 9. Comparison of the acoustic absorption coefficients for the assemblies with three- or single-layer of the perforated plates backed with airspaces.

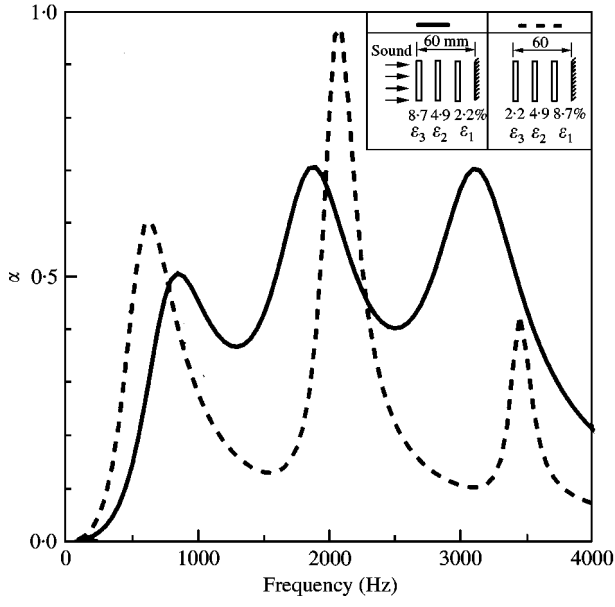


Figure 10. Comparison of the acoustic absorption coefficients for different arrangements of perforated plates.

different arrangements reveal three acoustic resonance frequencies at the discussed frequency bands (100–4000 Hz). As expected, the acoustic absorption for the case with porosity $\varepsilon_1 = 2{\cdot}2\%$, $\varepsilon_2 = 4{\cdot}9\%$ and $\varepsilon_3 = 8{\cdot}7\%$ is generally better than that with porosity $\varepsilon_1 = 8{\cdot}7\%$, $\varepsilon_2 = 4{\cdot}9\%$ and $\varepsilon_3 = 2{\cdot}2\%$ except at the frequency bands below 800 Hz and 2000–2300 Hz. This may be attributed to the fact that for the case with porosity $\varepsilon_1 = 2{\cdot}2\%$, $\varepsilon_2 = 4{\cdot}9\%$ and $\varepsilon_3 = 8{\cdot}7\%$, the incident sound can gradually enter the acoustic absorber and

be absorbed. However, for the case with porosity $\varepsilon_1 = 8{\cdot}7\%$, $\varepsilon_2 = 4{\cdot}9\%$ and $\varepsilon_3 = 2{\cdot}2\%$, the incident sound energy is almost reflected from the outermost perforated plates ($\varepsilon_3 = 2{\cdot}2\%$) except near the acoustic resonance frequency bands; therefore, the acoustic absorption is largely reduced at the frequency bands away from the acoustic resonance frequency. Besides, since the incident sound encounters the outermost layer of the perforated plates ($\varepsilon_3 = 2{\cdot}2\%$) first, the acoustic absorption at the first resonance frequency band is more distinct as compared with the other case of $\varepsilon_1 = 2{\cdot}2\%$. Similar phenomena are also noted for the third resonance frequency band occurring in the perforated plates with porosity $\varepsilon_3 = 8{\cdot}7\%$ and $\varepsilon_1 = 8{\cdot}7\%$. But for the second resonance frequency band induced by the middle perforated plate, the more profound sound energy reflected from the perforated plate ($\varepsilon_3 = 2{\cdot}2\%$) will enhance the acoustic absorption. Hence, the acoustic absorption at the second resonance frequency band for the case with porosity $\varepsilon_1 = 8{\cdot}7\%$, $\varepsilon_2 = 4{\cdot}9\%$ and $\varepsilon_3 = 2{\cdot}2\%$ is relatively promoted.

### 6.4. EFFECT OF POROUS MATERIALS

For studying the effect of the porous materials on the acoustic absorption, both the glass fiber material and airspace behind the perforated plate are estimated. The parameters of these two cases are shown in Figure 11. The flow resistivity and material constants of the porous material are $\sigma_1 = \sigma_2 = \sigma_3 = 16\,000\ \mathrm{N\,s/m^4}$ and $c_{1k} = 0{\cdot}0571$, $c_{2k} = -0{\cdot}754$, $c_{3k} = 0{\cdot}0891$, $c_{4k} = -0{\cdot}732$, $c_{5k} = 0{\cdot}189$, $c_{6k} = -0{\cdot}595$, $c_{7k} = 0{\cdot}0978$ and $c_{8k} = -0{\cdot}7$ ($k = 1$, 2 or 3) [2] respectively. From the results revealed in Figure 11, it is found that the glass fiber material will distinctly promote the acoustic absorption and shift the acoustic resonance frequencies to lower frequency bands. Such an effect of the glass fiber material on the acoustic absorption for the present assembly with three-layer perforated plates has also been discussed by Davern [4] for the assembly with single-layer perforated plate.

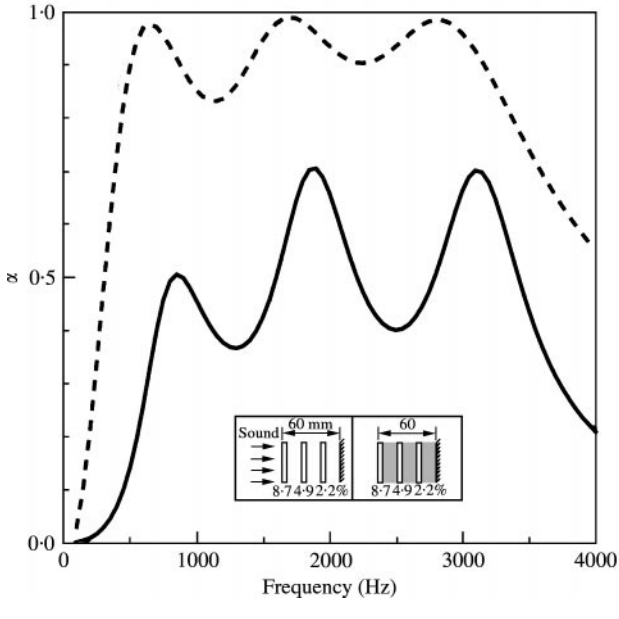


Figure 11. Comparison of the acoustic absorption coefficients for the perforated plates backed with airspaces or glass fiber materials: ——, air; - - - -, glass fiber.

## 7. CONCLUSIONS

In this work, the applicability and accuracy of the acoustic transmission analysis developed have been successfully demonstrated. By the present acoustic transmission analysis, the acoustic impedance and acoustic absorption coefficients for a realistic multi-layer acoustic absorber containing several compartments with perforated plates, airspaces and porous materials together can be calculated. The drawback of the equivalent electrical circuit approach in analyzing multi-layer acoustic absorbers, which always assumes the back surface acoustic impedance of airspaces or porous materials as that of the rigid wall, is compensated. Besides, several acoustic features of the multi-layer acoustic absorber are also discussed in detail. This provides a reliable guidance for the design of multi-layer acoustic absorbers.

## REFERENCES

1. L. L. BERANEK and I. L. VÉR 1992 *Noise and Vibration Control Engineering*, 232–243. New York: John Wiley and Sons; Chapter 8.
2. M. E. DELANY and E. N. BAZLEY 1970 *Applied Acoustics* **3**, 105–116. Acoustic properties of fibrous absorbent material.
3. W. QUNLI 1988 *Applied Acoustics* **25**, 141–148. Empirical relations between acoustic properties and flow resistivity of porous plastic open-cell foam.
4. W. A. DAVERN 1977 *Applied Acoustics* **10**, 85–112. Perforated facings backed with porous materials as sound absorbers—an experimental study.
5. I. P. DUNN and W. A. DAVERN 1986 *Applied Acoustics* **19**, 321–334. Calculation of acoustic impedance of multi-layer absorbers.
6. L. JINKYO, W. GEORGE and J. SWENSON 1992 *Noise Control Engineering Journal* **38**, 109–117. Compact sound absorbers for low frequencies.
7. M. L . MUNJAL 1987 *Acoustics of Ducts and Mufflers*, 53–88. New York: John Wiley and Sons; Chapter 2.
8. J. Y. CHUNG and D. A. BLASER 1980 *Journal of the Acoustic Society of America* **68**, 907–913, 914–921. Transfer function method of measuring in-duct acoustic properties. I: theory, II: experiment.
9. W. H. CHEN, F. C. LEE and D. M. CHIANG 2000 *Journal of Sound and Vibration* **237**, 337–355. On the acoustic absorption of porous materials with different surface shapes and perforated plates.
10. D. F. ROSS 1981 *Journal of Sound and Vibration* **79**, 133–143. A finite element analysis of perforated compartment acoustic systems.
11. V. EASWARAN and M. L. MUNJAL 1993 *Journal of Sound and Vibration* **160**, 333–350. Finite element analysis of wedges used in anechoic chambers.